Electronic Supplementary Material (ESI) for Soft Matter.

Supporting Information: Implications of protein polymorphism on protein phase behaviour

J. Stegen[1,2] and P. van der Schoot[1,2]

[1)] *Applied Physics, Eindhoven University of Technology, Eindhoven, 5600 MB, The Netherlands*

[2)] *Institute for Theoretical Physics, Utrecht University, Leuvenlaan 4, 3584 CE, Utrecht, The Netherlands*

(Dated: 29 December 2014)

I. SYMBOL LIST

ϕ - Protein volume-fraction.

η - Number-fraction of proteins in the non-native state.

η_{eq} - Equilibrium number-fraction of proteins in the non-native state.

$\phi_{\eta_{\mathrm{eq}}}$ - Equilibrium protein volume-fraction for a given value of η_{eq}.

$\mathrm{k_B}$ - Boltzmann constant.

T - Temperature.

χ - Dimensionless free energy (scaled on thermal energy, $\mathrm{k_BT}$) expressing the strength of attractive interaction between pairs of nearby proteins in the non-native state.

ϵ - Dimensionless free energy difference (scaled to thermal energy, $\mathrm{k_BT}$) between the native and the non-native state.

N - Number of proteins in the dispersion.

v_0 - Volume of a single protein.

f - Dimensionless free energy density scaled to the volume of a single protein, v_0, and in units of thermal energy, $\mathrm{k_BT}$.

f_{entr} - Entropic contribution to the dimensionless free energy density of the two-state protein model.

f_{enth} - Enthalpic contribution to the dimensionless free energy density of the two-state protein model.

f_{2s} - Dimensionless free energy density of the two-state protein model.

f_{FH} - Dimensionless free energy density of the Flory-Huggins-based solution model.

f_{CS} - Dimensionless free energy density of the Carnahan-Starling solution model.

f_{2sFH} - Dimensionless free energy density of the Flory-Huggins-based solution model and the two-state protein model combined.

f_{2sCS} - Dimensionless free energy density of the Carnahan-Starling solution model and the two-state protein model combined.

μ - Dimensionless chemical potential (scaled to thermal energy, $\mathrm{k_BT}$).

r_t - Ratio of self-diffusion time scale of a protein and the time scale at which conformational changes occur in a protein.

$\Delta\phi_S$ - Width of the concentration interval for which phase separation occurs by spinodal decomposition in a solution of initially native proteins.

II. CONDITIONS FOR THE EXISTENCE OF THE FIRST-ORDER CONFORMATIONAL PHASE TRANSITION

In section III a relation, given by eq. (4) , between the equilibrium fraction of proteins in the non-native state, η_{eq}, and protein concentration, ϕ, and the energetic parameters χ, giving the strength of interactions between proteins in the non-native state, and ϵ, which is the free energy penalty associated with the non-native state was derived. Furthermore, we showed there that this relation predicts the existence of a van der Waals-like loop separating dispersion states with proteins mostly in their native and proteins mostly in their non-native state by a first-order conformational phase transition.

Here, we investigate under which conditions this van der Waals-like loop and the phase transition exists. To do so, we rewrite eq. (4) to yield an explicit solution for the protein concentration as a function of η_{eq},

$$\phi_{\eta_{\mathrm{eq}}} = \frac{1}{\chi\eta_{\mathrm{eq}}}\left[\ln\left(\frac{\eta_{\mathrm{eq}}}{1-\eta_{\mathrm{eq}}}\right)+\epsilon\right]. \tag{1}$$

This relation is plotted for $\chi = 10$ $\mathrm{k_BT}$ and $\epsilon = 3$ $\mathrm{k_BT}$ in fig. 2b . From this figure it is clear that concentration-interval where the van der Waals-like loop is observed corresponds to the region bound by the points corresponding to a maximum and minimum in $\phi_{\eta_{\mathrm{eq}}}(\eta)$. These points obey $\partial_{\eta_{\mathrm{eq}}}\phi_{\eta_{\mathrm{eq}}} = 0$, which can be rewritten to yield a relation between the value of η_{eq} at these extrema as a function of ϵ,

$$\epsilon = \ln\left(\frac{1-\eta_{\mathrm{eq}}}{\eta_{\mathrm{eq}}}\right)+\frac{1}{1-\eta_{\mathrm{eq}}}. \tag{2}$$

This equation has a minimum of $\epsilon = 2$ at $\eta = 0.5$, meaning that $\epsilon = 2$ is the smallest free energy difference between the native and non-native state for which the van der Waals-like loop exists. Substitution of $\epsilon = 2$ and $\eta_{\mathrm{eq}} = 0.5$ into eq. (1) yields $\phi_{\eta_{\mathrm{eq}}} = 4/\chi$, so the lowest value of χ for $\epsilon = 2$ for which the van der Waals-like loop is observed, that is for $\phi_{\eta_{\mathrm{eq}}} = 1$, is $\chi = 4$.

For larger values of ϵ, the minimum value of χ for which the loop is observed must be determined numerically. Given a value of ϵ, the corresponding two values of η_{eq} bounding the van der Waals-like loop, must be determined by numerically solving eq. (2). Subsequently, one must numerically solve eq. (1) for $\phi_{\eta_{\mathrm{eq}}} = 1$, using the larger of the two previously determined values of η_{eq}, to determine the value of χ for which the loop is first observed for $\phi_{\eta_{\mathrm{eq}}} \leq 1$.

The presence of the (partial) van der Waals-like loop does not guarantee the existence of the first-order conformational phase transition. The first order conformational phase transition occurs between two dispersion states at equal concentration and free energy, but different average protein conformation, η. For any $\epsilon \geq 2$, it is first observed for $\chi = 2\epsilon$ when there is an Ising-like coexistence between dispersion states of different average protein conformation and of equal free energy at a concentration of $\phi = 1$. This point coincides with the critical "point" for liquid-liquid phase separation for the given value of ϵ.

III. SUPPORTING FIGURES AND TABLES

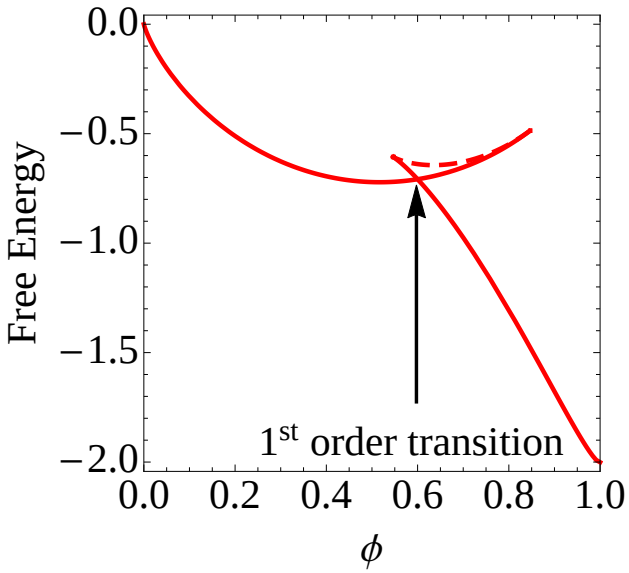

FIG. 1: The dimensionless Flory-Huggins-based free energy density along the η_{eq} curve, as shown in fig. 2b. The location of the first-order conformational phase transition is indicated. Furthermore, this figure shows that the van der-Waals like loop as shown in fig. 2b leads to a similar type of loop in the dimensionless free energy density.

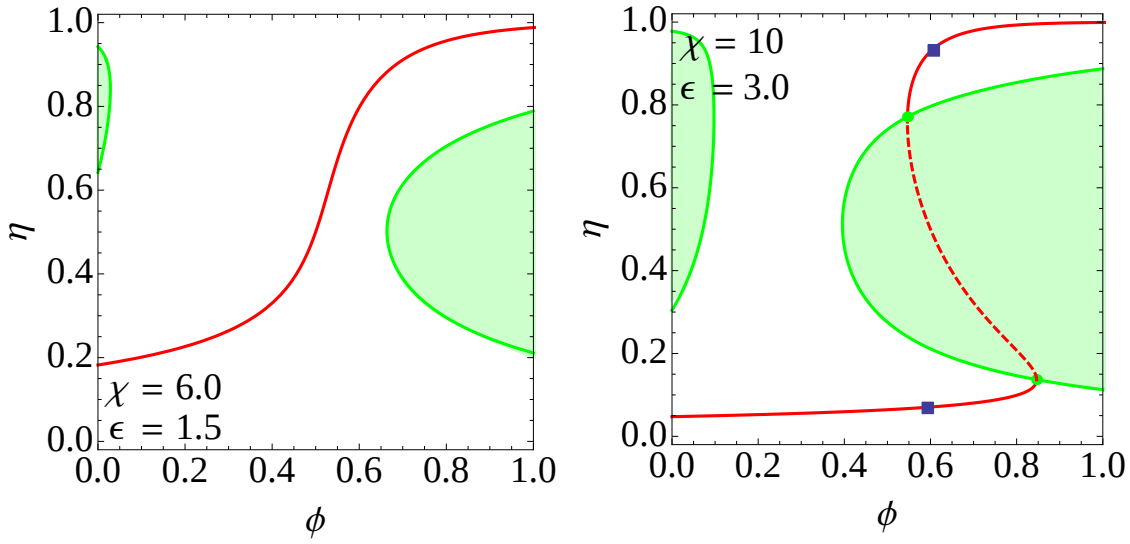

FIG. 2: See fig. 3, same plots but now for the Carnahan-Starling-based free energy. a) Unlike the Flory-Huggins-based free energy no phase separation occurs for $\chi = 6$ and $\epsilon = 1.5$ for the Carnahan-Starling-based free energy. b) For $\chi = 10$ and $\epsilon = 3$ phase separation can occur. The location of "equilibrium" spinodal points and binodal points is different from their position for the Flory-Huggins-based free energy.

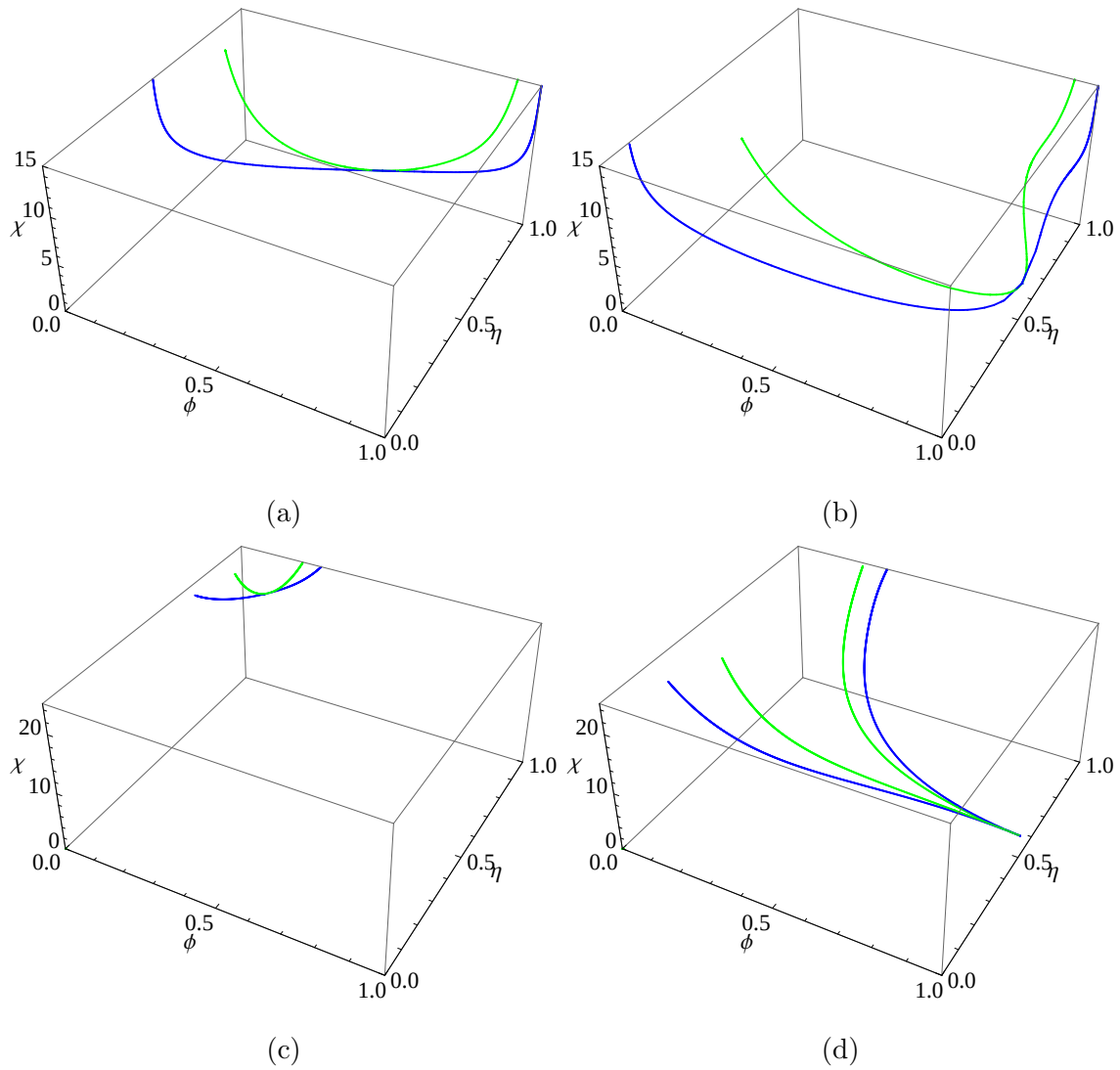

FIG. 3: Phase and stability diagrams for our two-state protein model as a function of the interaction parameter χ, protein volume fraction ϕ and average protein conformation η. The binodal is depicted as a blue line, the spinodal is given by the green line. a) Results from Flory-Huggins-based model for free energy difference between native and non-native states of $\epsilon = 0$ in units of thermal energy. b) Flory-Huggins-based model for $\epsilon = 2$. c) Carnahan-Starling-based model for $\epsilon = 0$. d) Carnahan-Starling-based model for $\epsilon = 2$.

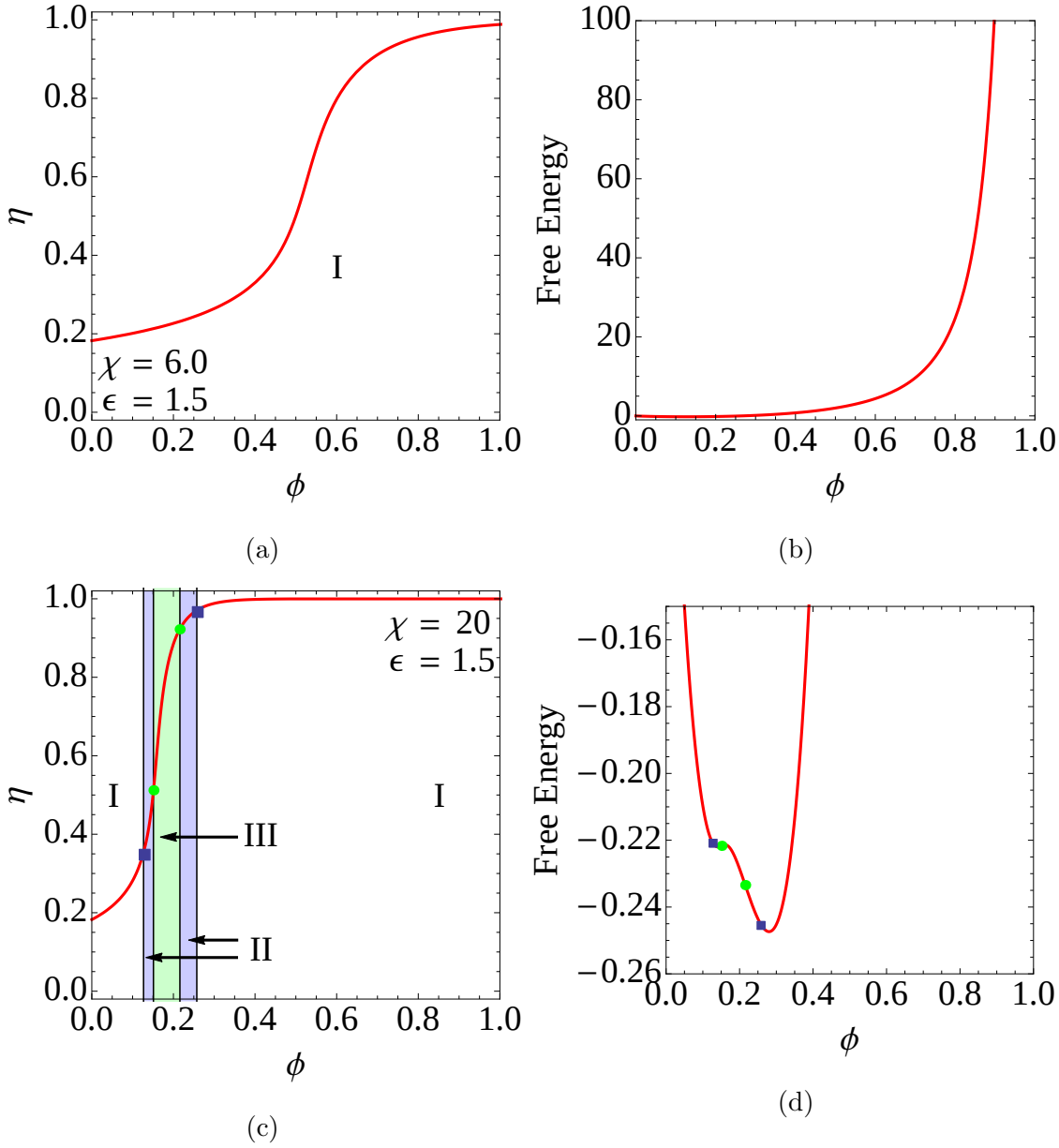

FIG. 4: a) The equilibrium fraction of proteins in the non-native state, $\eta_{\rm eq}$, as a function of ϕ for $\chi = 6$ and $\epsilon = 1.5$ calculated from the Carnahan-Starling based model. Unlike the Flory-Huggins-based model, no phase separation occurs for these values of the energetic parameters. b) Dimensionless Carnahan-Starling-based free energy density along the $\eta_{\rm eq}$ curve for $\chi = 6$ and $\epsilon = 1.5$, as a function of ϕ. c) same plot as a but for $\chi = 20$ and $\epsilon = 1.5$, now phase separation does occur, "equilibrium" spinodal points are shown as green dots and binodal points as blue squares. Regions I, II and III are defined as in fig. 4.

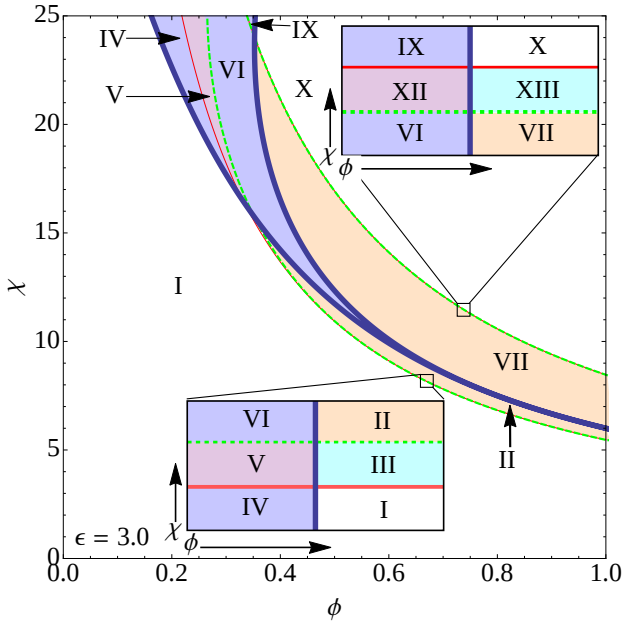

FIG. 5: The phase and stability diagram for $\epsilon = 3$ for the Carnahan-Starling-based free energy. The blue line represents the binodal, coexisting states are joined by horizontal tie-lines, the green dotted line represents the spinodal. Ten regions, each with distinct phase behaviour are indicated, but with identical behaviour as the same regions for the Flory-Huggins based free energy. Regions VIII, IX and XI are located at higher values of χ and not shown here. A 3D version of the diagram is shown in fig. S-5b.

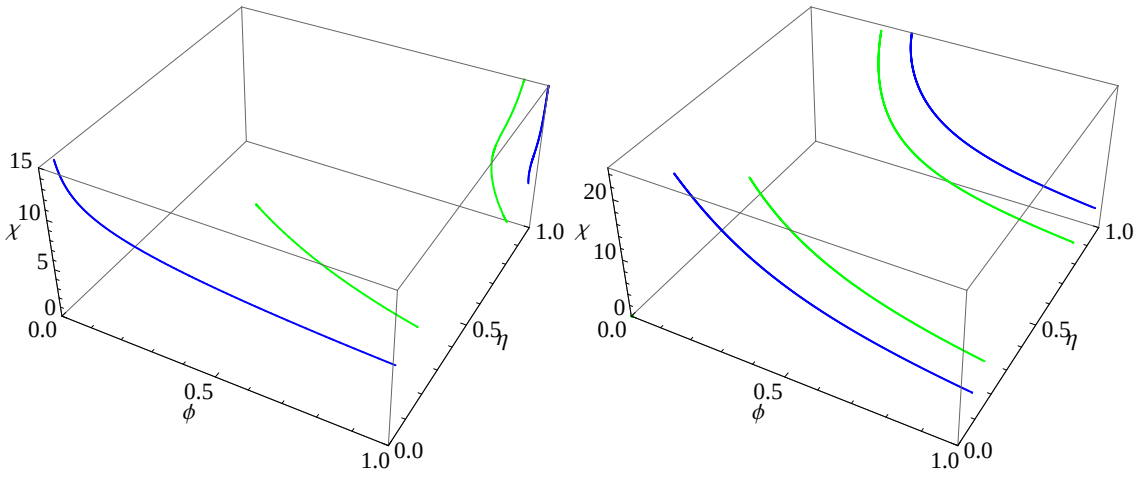

(a) (b)

FIG. 6: 3D phase and stability diagrams for $\epsilon = 3$. The blue line represents the binodal, coexisting states are joined by tie-lines at constant χ. The green line represents the spinodal. Note that there is no real critical point, at $\chi = 6$ there are two phases in Ising-like coexistence at $\phi = 1$ with different average protein conformation. a) Diagram for the Flory-Huggins-based free energy. b) Diagram for the Carnahan-Starling-based free energy.

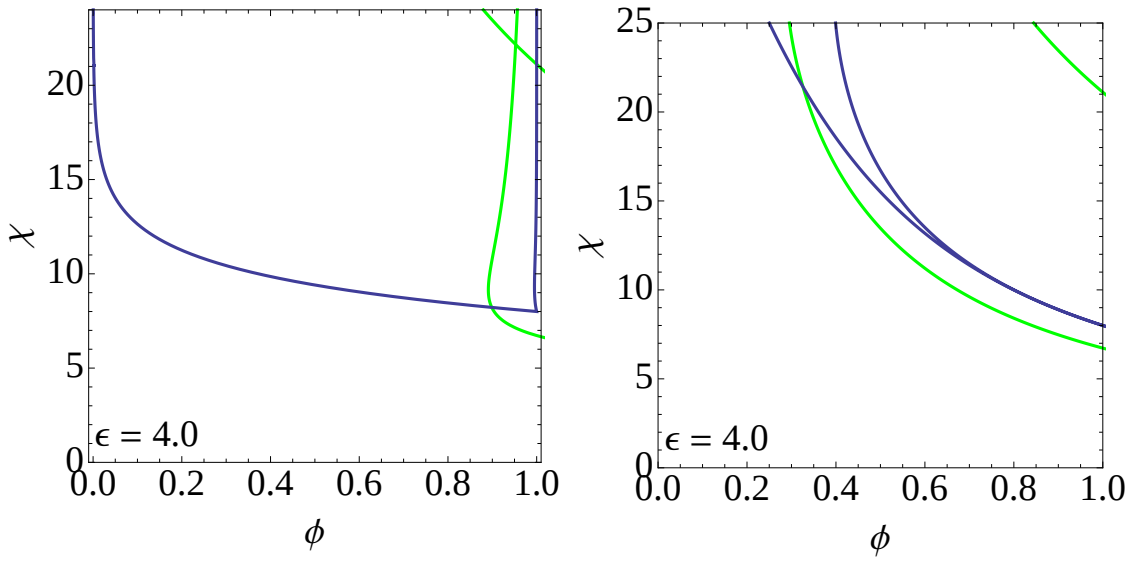

(a) (b)

FIG. 7: Phase and stability diagrams for $\epsilon = 4$ for a) the Flory-Huggins based free energy and b) the Carnahan-Starling based free energy. The blue line represents the binodal, coexisting states are joined by tie-lines at constant χ. The green line represents the spinodal. Note that these diagrams have been projected onto the ϕ-χ plane and the η dimension is not shown. The structure of the diagrams is identical to that for $\epsilon = 3.0$ as shown in fig. 6 and fig. S-4, however it has shifted to increased values of χ and some features of the diagram are not visible for the shown values of χ.

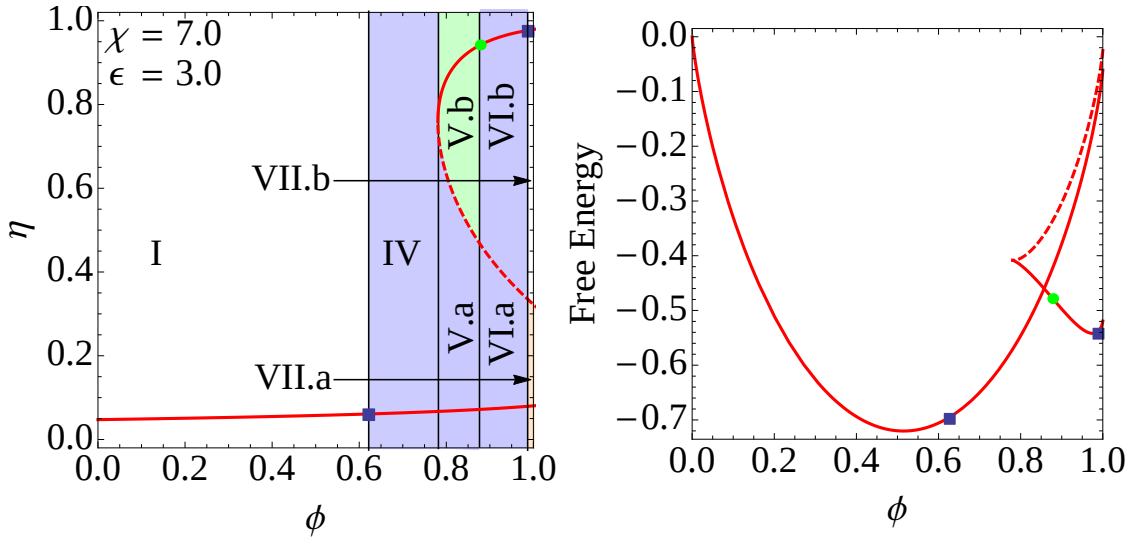

(a) (b)

FIG. 8: a) Mapping of phase behaviour in ϕ-η space for $\chi = 7$ and $\epsilon = 3.0$ for the Flory-Huggins-based free energy, showing the η_{eq} curve (red), "equilibrium" spinodal point (green dot). The regions denoted in the figure are situated in the corresponding regions in fig. 6, the behaviour in each of these regions is summarised in table S-1. b) The dimensionless Flory-Huggins-based free energy density along the η_{eq} curve for $\chi = 7$ and $\epsilon = 3.0$.

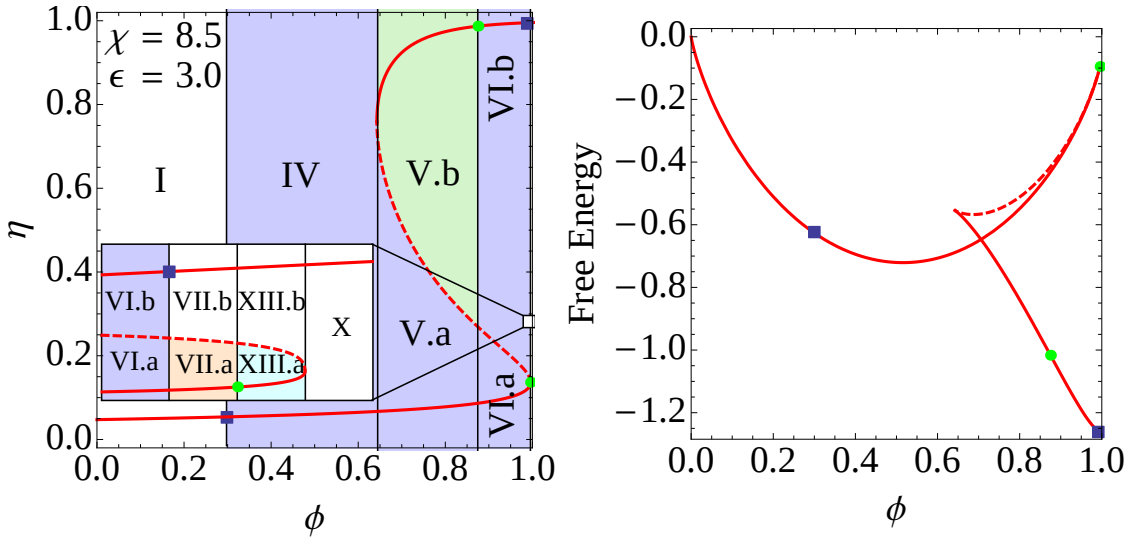

(a) (b)

FIG. 9: a) Mapping of phase behaviour in ϕ-η space for $\chi = 8.5$ and $\epsilon = 3.0$ for the Flory-Huggins-based free energy, showing the η_{eq} curve (red), "equilibrium" spinodal point (green dot). An inset schematically shows the rapid transition between different regions close to $\phi = 1$. The regions denoted in the figure are situated in the corresponding regions in fig. 6, the behaviour in each of these regions is summarised in table S-1. b) The dimensionless Flory-Huggins-based free energy density along the η_{eq} curve for $\chi = 8.5$ and $\epsilon = 3.0$.

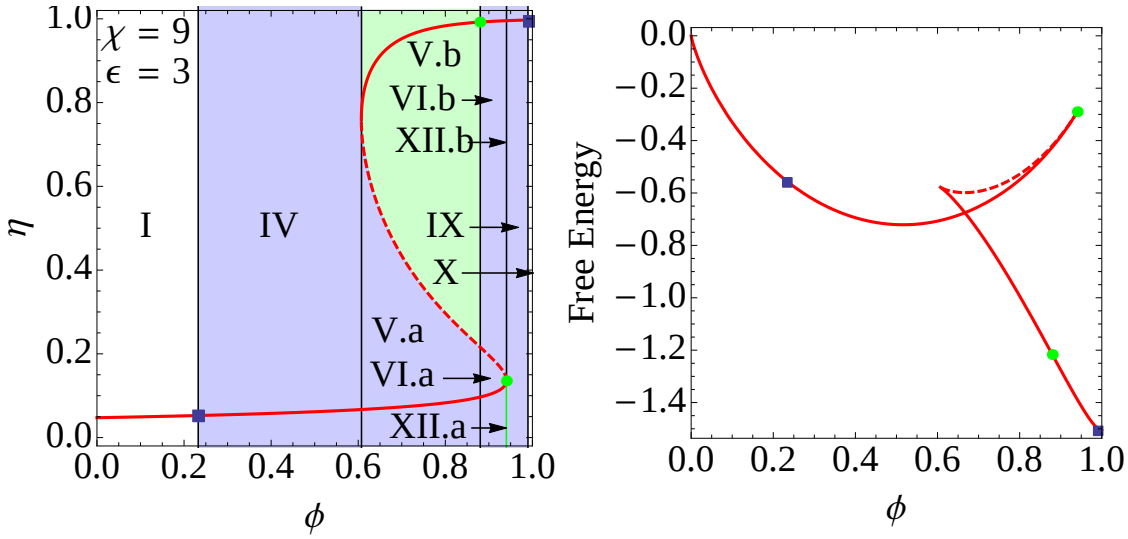

(a) (b)

FIG. 10: a) Mapping of phase behaviour in ϕ-η space for $\chi = 9$ and $\epsilon = 3.0$ for the Flory-Huggins-based free energy, showing the η_{eq} curve (red), "equilibrium" spinodal point (green dot). The regions denoted in the figure are situated in the corresponding regions in fig. 6, the behaviour in each of these regions is summarised in table S-1. b) The dimensionless Flory-Huggins-based free energy density along the η_{eq} curve for $\chi = 9$ and $\epsilon = 3.0$.

Region	a) Lower part of loop	b) Upper part of loop
I	Homogeneous	Homogeneous
II	Homogeneous	Meta-stable
III	Homogeneous	Meta-stable & spinodal decomposition
IV	Phase separation by nucleation and growth	Not present
V	Phase separation by nucleation and growth	Phase separation by spinodal decomposition
VI	Phase separation by nucleation and growth	Phase separation by nucleation and growth
VII	Meta-stable	Homogeneous
VIII	Not present	Phase separation by spinodal decomposition
IX	Not present	Phase separation by nucleation and growth
X	Not present	Homogeneous
XI	Phase separation by spinodal decomposition	Phase separation by spinodal decomposition
XII	Phase separation by spinodal decomposition	Phase separation by nucleation and growth
XIII	Meta-stable and spinodal decomposition	Homogeneous

TABLE I: Overview of phase and stability behaviour in regions I-XIII as shown in fig. 6 and fig. S-4. The lower part of the loop refers to the stable portion of the η_{eq} curve below the unstable part of the van der Waals-like loop while the upper part refers to part of the loop above it, see fig. 2b. Note that in region I the van der Waals-like loop in the η_{eq} curve does not exist.